HHS Public Access

Author manuscript

Am J Ophthalmol. Author manuscript; available in PMC 2018 July 03.

Published in final edited form as:

Am J Ophthalmol. 2016 April ; 164: 14–21. doi:10.1016/j.ajo.2015.12.020.

Discriminant Value of Custom Ocular Response Analyzer Waveform Derivatives in Forme Fruste Keratoconus

ALLAN LUZ, **BERNARDO LOPES**, **KATIE M. HALLAHAN**, **BRUNO VALBON**, **BRUNO FONTES**, **PAULO SCHOR**, **WILLIAM J. DUPPS JR**, and **RENATO AMBRÓSIO JR**

Department for Ophthalmology of the Federal University of Sao Paulo, Sao Paulo, Brazil (A.L., B.L., P.S., R.A.); Cole Eye Institute, Cleveland Clinic; and Biomedical Engineering, Cleveland Clinic Lerner Research Institute, Cleveland, Ohio (K.M.H., W.J.D.); Hospital de Olhos de Sergipe, Aracaju, Brazil (A.L.); Rio de Janeiro Corneal Tomography and Biomechanics Study Group, Rio de Janeiro, Brazil (A.L., B.L., B.V., R.A.); and Instituto de Olhos Renato Ambrósio and Visare Personal Laser, Rio de Janeiro, Brazil (B.L., B.V., B.F., R.A.)

Abstract

PURPOSE—To evaluate the performance of corneal hysteresis (CH), corneal resistance factor (CRF), 37 Ocular Response Analyzer (ORA) waveform parameters, and 15 investigator-derived ORA variables in differentiating forme fruste keratoconus (KC) from normal corneas.

DESIGN—Case-control study.

METHODS—Seventy-eight eyes of 78 unaffected patients and 21 topographically normal eyes of 21 forme fruste KC patients with topographically manifest KC in the contralateral eye were matched for age, the thinnest point of the cornea, central corneal thickness, and maximum keratometry. Fifteen candidate variables were derived from exported ORA signals to characterize putative indicators of biomechanical behavior, and 37 waveform parameters were tested. Differences between groups were assessed by the Mann-Whitney test. The area under the receiver operating characteristic curve (AUROC) was used to compare the diagnostic performance.

RESULTS—Ten of 54 parameters reached significant differences between the groups (Mann-Whitney test, $P < .05$). Neither CRF nor CH differed significantly between the groups. Among the ORA waveform measurements, the best parameters were those related to the area under the first peak, p1area, and p1area1 (AUROC, 0.714 ± 0.064 and 0.721 ± 0.065, respectively). Among the investigator ORA variables, a measure incorporating the pressure-deformation relationship of the entire response cycle performed best (hysteresis loop area, AUROC, 0.694 ± 0.067).

CONCLUSION—Waveform-derived ORA parameters, including a custom measure incorporating the pressure-deformation relationship of the entire response cycle, performed better than traditional CH and CRF parameters in differentiating forme fruste KC from normal corneas.

Ectasia is an important complication after refractive surgery, and there is interest in the preoperative identification of patients at risk for developing this condition.[1,2] A topographic keratoconus pattern is the most important risk factor.[3] A major goal of preoperative

Inquiries to Allan Luz, Jorge Amado Avenue 1500, Aracaju, SE, Brazil 49025 330; dr.allanluz@gmail.com.

evaluation is the detection of corneas with subclinical or early-stage keratoconus. Although clinical examination and computed corneal topography can be used to diagnose keratoconus in its clinical form, the detection of subclinical forms remains a challenge. Various terms, including keratoconus suspect and forme fruste keratoconus, have been used to describe the subclinical condition.[4]

The term “keratoconus suspect” was initially used to describe eyes at risk for developing keratoconus based on subjective impressions of topographic patterns. Videokeratography can be used to quantify the pattern of keratoconus and simplify the disease classification.[5] Using this approach, the progression of disease in keratoconus suspect eyes can be described using quantitative indices, and eyes with keratoconus can be confirmed.[6] Thus, the term keratoconus suspect can be reserved for corneas that display a topographic pattern characterized by specific quantitative indices. The term “forme fruste keratoconus” refers to topographic patterns that are insufficient to reach the threshold of keratoconus or keratoconus suspect based on computerized quantitative indices.[7]

Published studies have indicated that the corneal hysteresis (CH) value and corneal resistance factor (CRF) are lower in corneas with keratoconus and in corneas that have undergone laser in situ keratomileusis than in normal corneas.[8,9] In addition, new indices derived from the waveform signals obtained with an Ocular Response Analyzer (ORA; Reichert Ophthalmic Instruments, Depew, New York, USA) demonstrate the ability to distinguish keratoconus from normal corneas more accurately than the original pressure-derived parameters (CH, CRF).[10] A panel of candidate diagnostic variables using exported ORA data to characterize the temporal applanation signal intensity and the pressure features of the corneal response was also recently developed.[11]

Patients with topographically normal unilateral keratoconus provide a unique opportunity to evaluate methods for detecting the features of the disease at a very early stage. In the present study, we compared the original ORA pressure-derived parameters (CH, CRF, Goldman-correlated intraocular pressure [IOPg], corneal compensated intraocular pressure [IOPcc]), 37 waveform signal parameters, and 15 candidate variables from exported ORA signals to characterize putative indicators of biomechanical behavior between a group of fellow eyes of patients with unilateral keratoconus and a group of normal eyes. The groups were matched with regard to the central corneal thickness, the thinnest point of the cornea, and maximum keratometry (Kmax) in order to reduce the possibility of influencing the morphologic characteristics. The groups were also matched for age, which is known to affect the biomechanical results.[12]

METHODS

SUBJECTS

This study was a case-control study. The study protocol was approved by the Ethics and Research Committee of São Paulo Federal University (Protocol 2012/10), and a waiver of informed consent was granted because of the low risk of this research. The principles of the Declaration of Helsinki were followed for all study procedures.

Patients were examined at the Instituto de Olhos Renato Ambrósio (Rio de Janeiro, Brazil). We studied 99 eyes of 99 patients, who were divided into 2 groups: the case group, which comprised 21 eyes of 21 patients with normal Placido-disc corneal topographies, in which the fellow eye had keratoconus (forme fruste keratoconus cases); and the control group, which comprised 78 eyes of 78 patients with bilateral normal corneas. The control group was formed by randomly choosing a single eye of each patient with bilaterally normal eyes according to topographic criteria.

The criteria for normality and disease were based on the Rabinowitz indices and were evaluated by a corneal topographer using Placido disks (Humphrey Atlas). A KISA index greater than 100% was considered early keratoconus, a value less than 60% was considered normal, and values between 60% and 100% were considered suspect keratoconus. The fellow eye was considered for analysis when the KISA index on corneal topography was less than 60% without a suspect pattern.

The control group included patients without corneal topographic irregularities, high refractive error, or collagen vascular disease. Excluded from both groups were patients with severe ocular allergy, a history of ocular surgery or any eye disease, or any systemic disease or syndrome.

A comprehensive eye examination was conducted for all patients. In addition to the topographic data, the following information was obtained for each patient: age, thinnest point of the cornea, central pachymetry, topographic astigmatism, Kmax, and biomechanical data obtained with an ORA, including IOPg, IOPcc, CH, CRF, 37 parameters derived from analyses of the waveform signal, and 15 candidate variables using exported ORA data to characterize the temporal, applanation signal intensity, and pressure features of the corneal response. To avoid bias, patients allocated to each group were matched with regard to the thinnest point, maximum keratometry, age, and central pachymetry values, as these parameters influence the results obtained with an ORA.

PROCEDURES

To determine the ocular biomechanical properties, the ORA applies pressure to the cornea by focusing a pulsed jet of air on the eye, causing the cornea to pass through applanation and develop a slight concavity. Milliseconds after the initial applanation, the air pump that generated the pulse is turned off, and the pressure applied to the eye symmetrically decreases. As the pressure decreases, the cornea passes through a second applanated state while returning to its normal convexity.

Energy absorption during deformation of the cornea produces a difference in the signal peaks representing the first and second applanation events, indicating the difference between the pressures required for inward (loaded) and outward (unloaded) deformation of the cornea. This difference in applanation pressure is defined as CH, which indicates the viscous damping in the cornea and reflects the capacity of the corneal tissue to absorb and dissipate energy. CRF, a measure that was empirically derived as an indicator of the central corneal thickness, reflects the total corneal resistance, weighted towards elasticity.[13] In our study, only high-quality ORA readings were accepted for analysis.

With the introduction of new software (version 2.0), the ORA computes 37 new parameters that describe the waveform of the ORA response curve. The first set of these additional parameters describes the upper 75% of the peak height in the response curve with respect to the area under the curve (p1area, p2area); the upward slope (uslope1, uslope2), downward slope (dslope1, dslope2), width (w1, w2), height (h1, h2), and aspect ratio of the peaks (aspect1, aspect2); the path length around the peaks (path1, path2); the roughness of the peaks (aindex, bindex); and the roughness of the region between the peaks (aplhf), as well as 6 additional parameters (dive1, dive2, mslew1, mselw2, slew1, and slew2). A second set of parameters has the same description as the first set but considers only the upper 50% of the peak height (p1area1, p2area1, aspect11, aspect21, uslope11, uslope21, dslope11, dslope21, w11, w21, h11, h21, path11, path21). The p1area and p2area are influenced by the height of the infrared applanation signal peaks and the width (time course) of the corneal deformation response. The irregularity of the infrared signal peaks (aindex, bindex) and the roughness of the region between the peaks (aplhf) are related to the high-frequency components of the corneal deformation. Higher values indicate a more pronounced high-frequency/oscillatory corneal response.

ORA infrared intensity and pressure time series data were exported using ORA software and analyzed using custom Matlab routines (version 7.0; Math Works, Natick, Massachusetts, USA) as described previously.[11] Briefly, 15 variables were derived from the ORA signal and grouped according to waveform features as follows: applanation signal intensity (Group 1); applied pressure (Group 2); time (Group 3); applanation signal intensity as a function of the response time (Group 4); relationship between the applied pressure and the applanation signal response (Group 5); and relationship between the pressure and time (Group 6). All variables and their classifications are described in Table 1. Previously described investigator-derived variables defined using features of the ORA signal hypothesized to be biomechanically relevant were also calculated and are introduced in Figure 1.

The ORA calculates a waveform score that is used to select the best measurement value of each parameter out of the 4 measured.[14] We used the examination with the best waveform score after 4 consecutive measurements.

STATISTICAL ANALYSIS

Statistical analyses were performed using BioEstat 5.0 (Mamirauá Institute, Amazonas, Brazil) and MedCalc 11.1 (MedCalc Software, Mariakerke, Belgium). The nonparametric Mann-Whitney *U* test (Wilcoxon rank-sum) was used to evaluate the distribution of variables between the 2 groups. The significance criterion was submitted to Bonferroni correction. The receiver operating characteristic (ROC) curve and the area under the ROC curve (AUROC) were calculated for each parameter to examine the differences between the groups and determine the overall predictive accuracy of each test. The standard error of the AUROC was evaluated using the method of DeLong and associates.[15] The exact binomial method was used to calculate confidence intervals for AUROCs, with 0.700 indicating the cutoff point for poor parameter performance. Values of $P < .025$ were considered to indicate statistical significance.

RESULTS

Table 2 summarizes the demographic features, intra-ocular pressure, and topographic and tomographic characteristics of each group. The mean central pachymetry, thinnest point of the cornea, age, IOPg, IOPcc, astigmatism, and Kmax were not significantly different between the groups ($P > .05$). The mean KISA index was 17.86% (95% confidence interval [CI], 10.33%–25.39%) in the forme frusta keratoconus (FFKC) group and 11.77% (95% CI, 8.57%–14.96%) in the control group. Although the difference between the 2 groups was statistically significant ($P = .049$), the KISA index values were far below the 60% threshold for classification as keratoconus suspect based on the anterior topography features alone.

BIOMECHANICAL DATA

Table 3 compares the biomechanical parameters between the groups. Ten parameters differed significantly between the groups: *Pmax; Hysteresis Loop Area; Impulse; p1area; dive1; h1; p1area1; h11; uslope2; and mslew2*. Neither CH nor CRF achieved statistically significant differences.

The results of the ROC analysis demonstrated that parameters related to the area under the first peak (p1area and p1area1) achieved the best results for discriminating between the 2 groups, with sensitivities of 66.67% and 76.19%, specificities of 66.67% and 76.19%, and AUROCs of 0.714 and 0.721, respectively (Table 4). The five best-performing variables as determined by the highest AUROC values were as follows: *p1area1, p1area, Hysteresis Loop Area, h1*, and *h11*. Figure 2 illustrates the ROC performance of CH, p1area1, and Hysteresis Loop Area.

DISCUSSION

In our study, the populations of case and control eyes were comparable in age, thinnest point, central corneal thickness, maximum keratometry, and corneal astigmatism. Our goal was to control for morphologic characteristics (keratometry and pachymetry) that could influence the separation between the groups. There is no index in the classic screening that can distinguish between these 2 populations. Therefore, the differences found in this study are derived from differences in the latent biomechanical characteristics between the groups.

Because keratoconus is a bilateral, asymmetric ectatic degeneration, a patient with unilateral expression of the disease would be expected to have latent biomechanical instability in the other eye.[16] The incidence of true unilateral keratoconus is very low; the reported frequencies based on computerized videokeratography diagnosis techniques ranged from 0.5% to 4%.[17,18] Some studies have suggested that if patients are observed for a sufficient period of time, the signs of keratoconus will develop in the contralateral eye.[18,19] Detection of clinically advanced forms of keratoconus is not difficult, but the establishment of criteria to identify normal corneas with a susceptibility to the development of ectasia remains a challenge.[20] The topographically normal contralateral eye of a patient with unilateral keratoconus is a valuable investigational target for studying disease susceptibility prior to the development of clinical manifestations.[4]

This study provides insight into differences in the dynamic behavior of forme fruste keratoconus and normal eyes through analysis of novel waveform-derived candidate variables related to pressure, applanation, response time, or a combination of these variables. The forme fruste keratoconus eyes demonstrated the following characteristics: (1) marked reductions in a comprehensive hysteresis analog (Hysteresis Loop Area) that captures the pressure-deformation behavior of the entire response cycle; (2) reductions in the force and time required to reach the initial applanation; (3) a lower maximum air pressure intensity required to produce applanation as a function of the peak pressure and time; (4) a reduced area under the initial applanation intensity curve; (5) no difference in the high-frequency oscillation in the region between peaks and no difference in the corneal deformation from normal after an air puff; and (6) a lower speed of corneal deformation beyond applanation.

Our findings confirm prior results showing that the maximum applied pressure levels were significantly different between the FFKC and the normal eyes, with lower values for FFKC.[21] Additionally, a significantly lower intensity signal height at the first (inward) applanation peak was observed. In a previous study comparing the same custom variables in keratoconus and normal eyes, all variables except lag time were significantly different, and the minimum concavity and comprehensive measurement of hysteresis showed the greatest discriminate value for keratoconus.[11] In the present study, the AUROC for the hysteresis loop area was 0.694 (sensitivity 66.67% and specificity 71.79%). The AUROCs for impulse and Pmax were 0.654 and 0.652, respectively.

The hysteresis loop area provides an approximation of the classical mechanical concept of hysteresis, with the applied pressure being analogous to stress and the applanation signal intensity being analogous to strain. The hysteresis loop area reflects information about the cornea's response throughout the entire loading-unloading cycle.[11] Intraocular pressure has been shown to influence the cornea's biomechanical response, with a higher IOP correlated with a greater stiffness.[22] A previous study showed that the IOP has a minimal influence on the ORA custom variables.[11] The concern that IOP differences could confound the predictive value of key variables in the current study is minimized owing to the absence of statistically significant differences in IOPg and IOPcc between the groups (Table 2).

Multiple waveform oscillations could appear in ectatic eyes,[23] but this irregularity was not observed in this present FFKC study group. The parameters related to signal oscillation (path1, path11, path2, path21, aindex, and bindex) did not demonstrate statistically significant differences between the groups.

When analyzed independently, only 2 of 54 parameters achieved AUROC values above 0.700 in distinguishing FFKC from controls: p1area and p1area1 (AUROC = 0.714 and 0.721, respectively). A previous study also highlighted p1area, p1area1, p2area, and p2area1 for their performance in identifying grades I and II keratoconus.[24] In FFKC, by contrast, the present study demonstrated that only the areas related to the first applanation event were significant. Low values for p1area and p2area represented rapid applanation or applanation-recovery responses that are consistent with less viscous damping, but they may also reflect reduced applanation signal intensities owing to complex corneal surface deformation responses driven by heterogeneity in the properties of the corneal material. Because the

applanation signal height variables were significantly lower in the FFKC group in this study and the widths were not significantly different, it is most likely that the lower mean applanation signal height was responsible for the lower p1area in the FFKC group.

Previous studies have shown significant differences in the mean CH and CRF between keratoconic and normal corneas associated with a large overlap in the values of these parameters.[8,25] It has been postulated that waveform-derived variables may provide a greater discriminating ability for detecting early disease. Although we observed that certain waveform-derived variables had higher AUROC values than the original ORA variables, these variables were insufficient in our study as a sole criterion for the diagnosis of subclinical keratoconus in the absence of information about the disease state of the contralateral eye. This study was an exploratory analysis designed to restrict the initial number of candidate variables to a smaller subset of promising variables. The AUROC analysis was only performed on the variables in this subset to limit the potential impact of multiple comparisons on the results of the statistical analysis.

Many studies report methods of screening forme fruste keratoconus in the preoperative examination for corneal refractive surgery. Topographic examination remains the most frequently used and described method for screening such corneas. In recent years the ability to use tomographic evaluation to detect patients with susceptibility to developing ectasia has been enhanced.[26] Wavefront analysis revealing greater amounts of high-order aberrations, such as a third-order coma, provides yet another diagnostic tool for the identification of ectatic corneas.[27] Directly or indirectly, the aforementioned measurement modalities represent the corneal morphology rather than the corneal biomechanical properties. Newly developed devices, such as the Corvis ST (Oculus, Wetzlar, Germany), Brillouin scattering, [28] and optical coherence tomography–based deformation analysis techniques,[29] may allow for more direct measurement of the biomechanical properties and may offer additional sensitivity for detecting early ectatic predisposition.

In summary, differences in the derivatives of the dynamic corneal response to an air puff were observed between normal eyes and forme fruste keratoconus cases, despite similar corneal topographic measurements. This study confirms the importance of corneal biomechanical abnormalities in early ectatic disease. While these parameters cannot be used in isolation to detect mild ectasia, future studies to test their added value to topometric, tomographic, or wavefront-derived parameters are needed.

Supplementary Material

Refer to Web version on PubMed Central for supplementary material.

Acknowledgments

Funding/Support: No funding or grant support. financial disclosures: Renato Ambrosio: consultant of Oculus Optikgeräte GmbH. William Dupps: consultant of Ziemer and sponsored research and medical advisory board of Avedro. The following authors have no financial disclosures: Allan Luz, Bernardo Lopes, Katie M. Hallahan, Bruno Valbon, Bruno Fontes, and Paulo Schor. All authors attest that they meet the current ICMJE criteria for authorship.

References

1. Binder PS. Risk factors for ectasia after LASIK. J Cataract Refract Surg. 2008; 34(12):2010–2011. [PubMed: 19027544]
2. Randleman JB, Woodward M, Lynn MJ, Stulting RD. Risk assessment for ectasia after corneal refractive surgery. Ophthalmology. 2008; 115(1):37–50. [PubMed: 17624434]
3. Randleman JB, Trattler WB, Stulting RD. Validation of the Ectasia Risk Score System for preoperative laser in situ keratomileusis screening. Am J Ophthalmol. 2008; 145(5):813–818. [PubMed: 18328998]
4. Saad A, Gatinel D. Evaluation of total and corneal wavefront high order aberrations for the detection of forme fruste keratoconus. Invest Ophthalmol Vis Sci. 2012; 53(6):2978–2992. [PubMed: 22427590]
5. Klyce SD, Smolek MK, Maeda N. Keratoconus detection with the KISA% method-another view. J Cataract Refract Surg. 2000; 26(4):472–474. [PubMed: 10819626]
6. Klyce SD, Karon MD, Smolek MK. Screening patients with the corneal navigator. J Refract Surg. 2005; 21(5 Suppl):S617–S622. [PubMed: 16212291]
7. Klyce SD. Chasing the suspect: keratoconus. Br J Ophthalmol. 2009; 93(7):845–847. [PubMed: 19553507]
8. Fontes BM, Ambrosio R Jr, Jardim D, Velarde GC, Nose W. Corneal biomechanical metrics and anterior segment parameters in mild keratoconus. Ophthalmology. 2010; 117(4):673–679. [PubMed: 20138369]
9. Ortiz D, Pinero D, Shabayek MH, Arnalich-Montiel F, Alio JL. Corneal biomechanical properties in normal, post-laser in situ keratomileusis, and keratoconic eyes. J Cataract Refract Surg. 2007; 33(8): 1371–1375. [PubMed: 17662426]
10. Mikielewicz M, Kotliar K, Barraquer RI, Michael R. Air-pulse corneal applanation signal curve parameters for the characterisation of keratoconus. Br J Ophthalmol. 2011; 95(6):793–798. [PubMed: 21310802]
11. Hallahan KM, Sinha Roy A, Ambrosio R Jr, Salomao M, Dupps WJ Jr. Discriminant value of custom ocular response analyzer waveform derivatives in keratoconus. Ophthalmology. 2014; 121(2):459–468. [PubMed: 24289916]
12. Fontes BM, Ambrosio R Jr, Alonso RS, Jardim D, Velarde GC, Nose W. Corneal biomechanical metrics in eyes with refraction of −19.00 to +9. 00 D in healthy Brazilian patients. J Refract Surg. 2008; 24(9):941–945. [PubMed: 19044236]
13. Luce DA. Determining in vivo biomechanical properties of the cornea with an ocular response analyzer. J Cataract Refract Surg. 2005; 31(1):156–162. [PubMed: 15721708]
14. Luz A, Fontes BM, Lopes B, et al. Best waveform score for diagnosing keratoconus. Revista Brasileira de Oftalmologia. 2013; 72:361–365.
15. DeLong ER, DeLong DM, Clarke-Pearson DL. Comparing the areas under two or more correlated receiver operating characteristic curves: a nonparametric approach. Biometrics. 1988; 44(3):837–845. [PubMed: 3203132]
16. Kozobolis V, Sideroudi H, Giarmoukakis A, Gkika M, Labiris G. Corneal biomechanical properties and anterior segment parameters in forme fruste keratoconus. Eur J Ophthalmol. 2012; 22(6):920–930. [PubMed: 22865401]
17. Rabinowitz YS, Nesburn AB, McDonnell PJ. Videokeratography of the fellow eye in unilateral keratoconus. Ophthalmology. 1993; 100(2):181–186. [PubMed: 8437824]
18. Holland DR, Maeda N, Hannush SB, et al. Unilateral keratoconus. Incidence and quantitative topographic analysis. Ophthalmology. 1997; 104(9):1409–1413. [PubMed: 9307634]
19. Li X, Rabinowitz YS, Rasheed K, Yang H. Longitudinal study of the normal eyes in unilateral keratoconus patients. Ophthalmology. 2004; 111(3):440–446. [PubMed: 15019316]
20. Saad A, Lteif Y, Azan E, Gatinel D. Biomechanical properties of keratoconus suspect eyes. Invest Ophthalmol Vis Sci. 2010; 51(6):2912–2916. [PubMed: 20042662]

21. Schweitzer C, Roberts CJ, Mahmoud AM, Colin J, Maurice-Tison S, Kerautret J. Screening of forme fruste keratoconus with the ocular response analyzer. Invest Ophthalmol Vis Sci. 2010; 51(5):2403–2410. [PubMed: 19907025]
22. Huseynova T, Waring GO 4th, Roberts C, Krueger RR, Tomita M. Corneal biomechanics as a function of intraocular pressure and pachymetry by dynamic infrared signal and Scheimpflug imaging analysis in normal eyes. Am J Ophthalmol. 2014; 157(4):885–893. [PubMed: 24388837]
23. Kerautret J, Colin J, Touboul D, Roberts C. Biomechanical characteristics of the ectatic cornea. J Cataract Refract Surg. 2008; 34(3):510–513. [PubMed: 18299080]
24. Ventura BV, Machado AP, Ambrosio R Jr, et al. Analysis of waveform-derived ORA parameters in early forms of keratoconus and normal corneas. J Refract Surg. 2013; 29(9):637–643. [PubMed: 24016349]
25. Fontes BM, Ambrosio R Jr, Velarde GC, Nose W. Ocular response analyzer measurements in keratoconus with normal central corneal thickness compared with matched normal control eyes. J Refract Surg. 2011; 27(3):209–215. [PubMed: 20481414]
26. Ambrosio R Jr, Alonso RS, Luz A, Coca Velarde LG. Corneal-thickness spatial profile and corneal-volume distribution: tomographic indices to detect keratoconus. J Cataract Refract Surg. 2006; 32(11):1851–1859. [PubMed: 17081868]
27. Jafri B, Li X, Yang H, Rabinowitz YS. Higher order wavefront aberrations and topography in early and suspected keratoconus. J Refract Surg. 2007; 23(8):774–781. [PubMed: 17985796]
28. Scarcelli G, Pineda R, Yun SH. Brillouin optical microscopy for corneal biomechanics. Invest Ophthalmol Vis Sci. 2012; 53(1):185–190. [PubMed: 22159012]
29. Ford MR, Dupps WJ Jr, Rollins AM, Roy AS, Hu Z. Method for optical coherence elastography of the cornea. J Biomed Opt. 2011; 16(1):016005. [PubMed: 21280911]

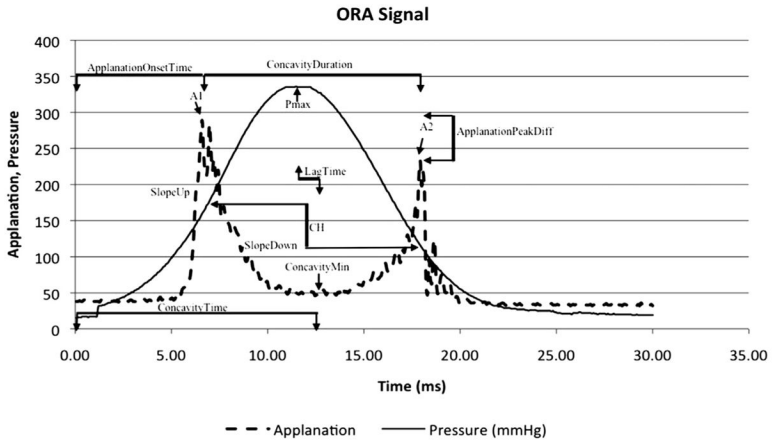

FIGURE 1.

Graphical representation of Ocular Response Analyzer (ORA) signal output with select variables from applanation signal intensity (A1, A2, Applanation peak difference and concavity min); pressure (Pmax); time (concavity duration, concavity time, and lag time); and applanation signal intensity as a function of response time (slope up and slope down).

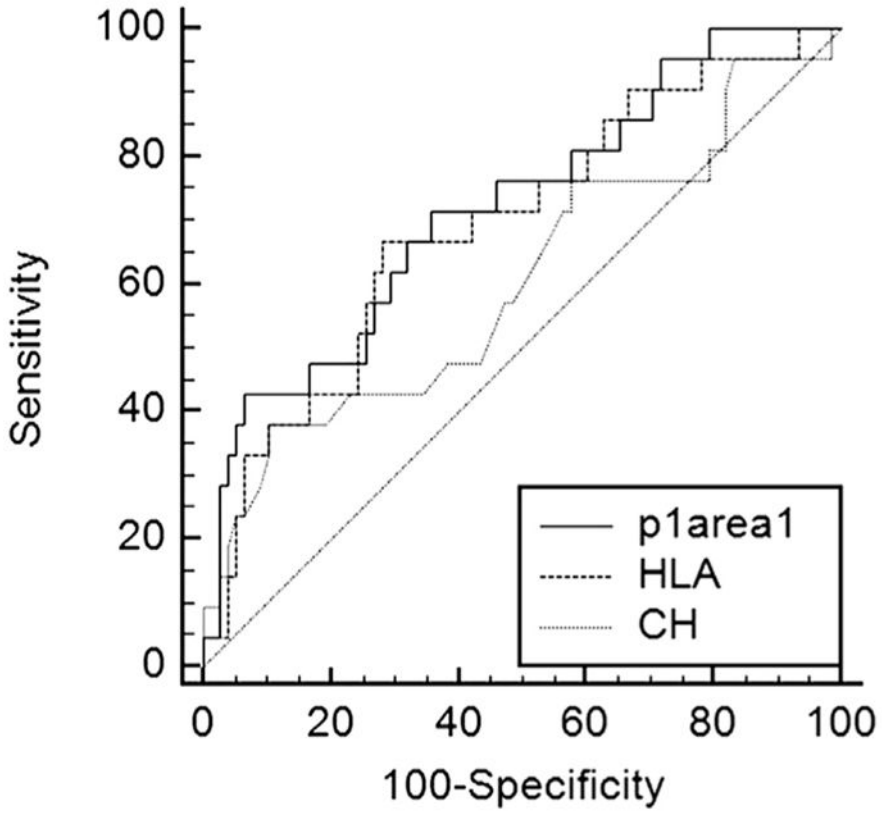

FIGURE 2.

Comparison of receiver operating characteristic (ROC) performance of corneal hysteresis (CH), p1area1, and hysteresis loop area (HLA) in discriminating forme fruste keratoconus from normal eyes.

TABLE 1

Ocular Response Analyzer Waveform Derivatives in Forme Fruste Keratoconus: Variables Derived From the Signal of the Dynamic Bidirectional Applanation Device (Adapted From Hallahan and Associates[11])

Variable	Operation Definition	Interpretation
Group 1		
A_1	Peak intensity of first applanation event	Maximum surface area achieving planarity during inward deformation
A_2	Peak intensity of second applanation event	Maximum surface area achieving planarity during recovery
Applanation peak difference	$A_2 - A_1$	Difference in maximum planarity between inward and recovery phases
Concavity min	Minimum applanation intensity between A1 and A2	Depth and irregularity (nonplanarity) of deformation
Concavity mean	Mean applanation intensity between A_1 and A_2	Depth and irregularity of deformation average
Group 2		
Average P1P2	(P1 + P2)/2	Average of the pressures at the 2 applanation events
Pmax	Peak value of pressure signal	Force and time required to reach fisrt applanation event
Group 3		
Concavity duration	Time lapse between A_1 and A_2	Temporal delay of deformation recovery between applanation events
Concavity time	Time from onset of applied pressure to A_1	Time required to achieve maximum deformation from onset of impulse
Lag time	Time between P_{max} and concavity min	Delay between peak applied pressure and maximum deformation
Applanation onset time	Time from onset of applied pressure to A_1	Time required to achieve first applanation from onset of impulse
Group 4		
Slope up	Positive slope of the first applanation peak, from inflection point to peak	Rate of achieving peak planarity
Slope down	Negative slope of the first applanation peak, from inflection point to peak	Rate of loss of peak planarity
Group 5		
Hysteresis loop area	Area enclosure by pressure versus applanation function	Hysteresis aggregated over entire deformation cycle except concavity
Group 6		
Impulse	Area under pressure versus time curve	Air pressure intensity

TABLE 2

Ocular Response Analyzer Waveform Derivatives in Forme Fruste Keratoconus: Comparison of Characteristics and Intraocular Pressure of Normal and Forme Fruste Keratoconus Groups

	FFKC Group	Control Group	*P* Value
Patients	21	78	-
Eyes	21	78	-
Age (y)	25.5 ± 7.2	26.6 ± 7.9	.2
Central pachymetry (mm)	527.3 ± 16.7	527.9 ± 23.4	.2
Thinnest point (mm)	526 ± 16.9	525.3 ± 23	.08
Astigmatism (D)	1.2 ± 0.8	1.4 ± 1.1	.1
Kmax (D)	44.9 ± 1.8	44.4 ± 1.4	.3
IOPg (mm Hg)	12.5 ± 2.8	13.9 ± 2.9	.08
IOPcc (mm Hg)	14.3 ± 3.4	14.8 ± 2.7	.3

D = diopter; FFKC = forme frusta keratoconus; IOPcc = corneal compensated intraocular pressure; IOPg = Goldmann intraocular pressure; Kmax = maximum keratometry.

TABLE 3

Ocular Response Analyzer Waveform Derivatives in Forme Fruste Keratoconus: Comparison of Custom Variables for Normal and Forme Fruste Keratoconus Groups

Parameter	Normal Mean ± SD	FFKC Mean ± SD	*P* Value
CRF	9.76 ± 1.76	9.10 ± 1.99	.0815
CH	10.14 ± 1.61	9.27 ± 2.16	.1375
AvgP1P2	176.38 ± 22.12	179.43 ± 55.85	.2099
Pmax	424.31 ± 35.23	408.43 ± 45.09	.0327
Concavity duration	10.90 ± 0.45	10.69 ± 1.14	.942
Concavity time	12.95 ± 0.88	12.83 ± 0.87	.5692
Lag time	0.81 ± 0.56	0.74 ± 0.50	.6409
Applanation onset time	7.69 ± 0.43	7.66 ± 0.77	.186
A1	585.42 ± 151.68	519.00 ± 160.57	.0926
A2	483.38 ± 136.40	418.38 ± 174.69	.1298
Applanation peak difference	−102.04 ± 126.51	−100.62 ± 169.75	.8877
Concavity min	48.89 ± 9.89	51.87 ± 12.44	.2427
Concavity mean	120.32 ± 21.66	117.94 ± 44.04	.2964
Slope down	−105.12 ± 36.30	−93.03 ± 38.26	.1504
Slope up	79.04 ± 30.07	66.57 ± 30.08	.2083
HLA	55570.78 ± 15835.89	43614.55 ± 18597.56	.0067*[a]
Impulse	4541.11 ± 320.55	4402.86 ± 418.84	.031
p1area	3351.49 ± 907.78	2644.83 ± 746.93	.0027*[a]
aspect1	18.06 ± 6.18	15.34 ± 6.19	.0985
uslope1	63.31 ± 31.53	49.71 ± 25.17	.075
dslope1	26.19 ± 8.87	23.25 ± 9.42	.1504
w1	21.59 ± 2.68	21.71 ± 3.51	.6439
dive1	324.06 ± 119.49	266.39 ± 115.82	.0395
h1	379.39 ± 104.01	319.06 ± 102.74	.019*[a]
path1	22.43 ± 3.94	24.96 ± 6.05	.1193
mslew1	106.45 ± 39.14	89.58 ± 30.31	.0779
slew1	64.77 ± 31.04	56.41 ± 25.13	.4161
p1area1	1416.89 ± 442.61	1085.19 ± 363.43	.0019[a]
Aindex	9.24 ± 1.04	8.59 ± 1.52	.0909
aspect11	24.52 ± 9.82	25.29 ± 16.21	.5491
uslope11	62.03 ± 31.47	56.78 ± 31.67	.4113
dslope11	41.04 ± 17.51	44.78 ± 27.95	.9532
w11	11.01 ± 2.43	10.05 ± 3.25	.2275
h11	252.93 ± 69.34	212.70 ± 68.49	.019*[a]
path11	32.61 ± 7.16	36.11 ± 9.16	.0736
Aplhf	1.31 ± 0.31	1.55 ± 0.84	.1933
p2area	2193.56 ± 593.84	1928.98 ± 597.38	.179

Parameter	Normal Mean ± SD	FFKC Mean ± SD	*P* Value
aspect2	18.16 ± 8.99	14.54 ± 11.03	.067
uslope2	85.64 ± 43.11	62.14 ± 45.55	.048
dslope2	23.63 ± 12.91	19.51 ± 14.99	.0869
w2	18.59 ± 4.52	22.67 ± 9.02	.1153
h2	305.88 ± 94.65	252.13 ± 120.12	.0689
dive2	236.13 ± 88.24	209.27 ± 111.58	.4386
path2	25.53 ± 6.57	25.33 ± 6.05	.9863
mslew2	127.26 ± 56.25	97.08 ± 51.35	.0452
slew2	86.04 ± 42.52	63.70 ± 44.10	.05
p2area1	930.90 ± 282.29	831.18 ± 277.80	.3464
aspect21	26.30 ± 14.23	20.85 ± 15.21	.1012
uslope21	68.73 ± 31.87	54.66 ± 42.13	.0869
dslope21	41.18 ± 26.53	32.25 ± 24.35	.1433
w21	9.00 ± 3.02	10.67 ± 5.31	.4088
h21	203.92 ± 63.10	168.09 ± 80.08	.0689
path21	36.07 ± 9.27	34.00 ± 8.43	.3553
Bindex	9.35 ± 1.07	8.42 ± 2.32	.2194

CH = corneal hysteresis; CRF = corneal resistance factor; FFKC = forme frusta keratoconus; HLA = hysteresis loop area.

Asterisk indicates significant results.

[a]Mann-Whitney *U* test with Bonferroni correction.

TABLE 4

Ocular Response Analyzer Waveform Derivatives in Forme Fruste Keratoconus: Comparison of Area Under the Receiver Operating Characteristic Curve, Select Parameter Cutoff, Sensitivity, and Specificity for Variables Statistically Different Between Normal and Forme Fruste Keratoconus Groups

Parameter	AUROC	SE	*P* Value	Sensitivity	Specificity	Cutoff	95% CI
p1area1	0.721	0.0651	.0007	76.19	53.85	≤1301.5	0.622–0.806
p1area	0.714	0.0637	.0008	66.67	60.26	≤2968.5	0.615–0.801
HLA	0.694	0.0674	.0041	66.67	71.79	≤49903	0.593–0.782
h1	0.667	0.0703	.0174	61.9	69.23	≤319.68	0.565–0.759
h11	0.667	0.0703	.0174	61.9	69.23	≤213.12	0.565–0.759
Impulse	0.654	0.0699	.0278	71.43	60.26	≤4442.5	0.552–0.747
Pmax	0.652	0.0688	.0268	61.9	65.38	≤413	0.550–0.745
dive1	0.647	0.0679	.0306	61.9	62.82	≤279	0.544–0.740
mslew2	0.643	0.0701	.0416	52.38	70.51	≤95.5	0.540–0.737
uslope2	0.641	0.0765	.0651	57.14	69.23	≤65.5	0.538–0.735

AUROC = area under the receiver operating characteristic curve; HLA = hysteresis loop area.